

## ORIGINAL ARTICLE

USP4 inhibits p53 and NF- $\kappa$ B through deubiquitinating and stabilizing HDAC2Z Li<sup>1,2,8</sup>, Q Hao<sup>1,2,8</sup>, J Luo<sup>3,8</sup>, J Xiong<sup>1,2,8</sup>, S Zhang<sup>4</sup>, T Wang<sup>1</sup>, L Bai<sup>5</sup>, W Wang<sup>2</sup>, M Chen<sup>2</sup>, W Wang<sup>2</sup>, L Gu<sup>2</sup>, K Lv<sup>6,7</sup> and J Chen<sup>2</sup>

Histone deacetylases (HDACs) are major epigenetic modulators involved in a broad spectrum of human diseases including cancers. As HDACs are promising targets of cancer therapy, it is important to understand the mechanisms of HDAC regulation. In this study, we show that ubiquitin-specific peptidase 4 (USP4) interacts directly with and deubiquitinates HDAC2, leading to the stabilization of HDAC2. Accumulation of HDAC2 in USP4-overexpression cells leads to compromised p53 acetylation as well as crippled p53 transcriptional activation, accumulation and apoptotic response upon DNA damage. Moreover, USP4 targets HDAC2 to downregulate tumor necrosis factor TNF $\alpha$ -induced nuclear factor (NF)- $\kappa$ B activation. Taken together, our study provides a novel insight into the ubiquitination and stability of HDAC2 and uncovers a previously unknown function of USP4 in cancers.

Oncogene (2016) 35, 2902–2912; doi:10.1038/onc.2015.349; published online 28 September 2015

## INTRODUCTION

Acetylation and deacetylation of histone proteins play an important role in chromatin remodeling and transcriptional regulation.<sup>1</sup> Two groups of corresponding enzymes, histone deacetylases (HDACs) and histone acetyl-transferases, act in concert to maintain the balance between condensed and relaxed chromatin by catalyzing the removing or adding of acetyl groups to specific lysine-rich amino terminal histone residues.<sup>2,3</sup> Hyperacetylation of the N terminus of histone tails induced by histone acetyl-transferases correlates with gene activation, whereas deacetylation by HDACs has been shown to mediate transcriptional suppression.<sup>4</sup> Consequently, HDACs play critical roles in cellular growth, differentiation, apoptosis and transformation; dysregulation of acetylation status in the cell is closely linked to cancer.<sup>5</sup>

HDACs have been classified into different subfamilies based on phylogenetic analysis and sequence homology in mammals.<sup>2</sup> Class I deacetylases (HDACs 1, 2, 3 and 8) are ubiquitously expressed enzymes that show the strongest HDAC activity that deacetylate both histone and nonhistone proteins *in vitro* and *in vivo*. Class IIa (HDACs 4, 5, 7 and 9) and IIb (HDACs 6 and 10) enzymes are larger and their expression is restricted to certain cell types. HDAC11 belongs to class IV. Sirtuins, mammalian orthologs of yeast Sir2, comprise class III (SIRT1–7).<sup>6–8</sup>

In addition to histones, several nonhistone targets of HDACs such as p53, E2F1, STAT1, STAT3 and nuclear factor (NF)- $\kappa$ B have been identified.<sup>9</sup> The best example is the tumor suppressor p53.<sup>10–13</sup> p53, often regarded as the 'guardian of the genome', exerts tumor suppressive capacities by centrally coordinating a regulatory circuit that monitors and responds to a variety of stress signals, including DNA damage, abnormal oncogenic events, telomere erosion and hypoxia.<sup>14,15</sup> Upon stress, p53 is acetylated

and phosphorylated, followed by its accumulation and its transcriptional activation of p21, MDM2, Bax, Puma and Noxa because of its dissociation from its ubiquitin ligase, MDM2,<sup>16–21</sup> subsequently leading to cell cycle arrest and apoptosis.<sup>22</sup> The acetylation of p53 is regulated by histone acetyl-transferases and HDACs.<sup>10–13,23,24</sup> Both HDAC1 (class I) and SIRT1 (class III) were reported to deacetylate p53, resulting in transcriptional inhibition.<sup>10,25</sup> More recently, HDAC1 and HDAC2 were shown to suppress p53 hyperacetylation in embryonic epidermis.<sup>26</sup> The transactivation function of NF- $\kappa$ B is also regulated through interaction of the p65 (RelA) subunit with HDACs. HDAC1 and HDAC2 target NF- $\kappa$ B through a direct association of HDAC1 with the Rel homology domain of p65. HDAC2 does not interact with NF- $\kappa$ B directly but can regulate NF- $\kappa$ B activity through its association with HDAC1.<sup>27</sup> HDAC1/2 was also reported to regulate the acetylation state of NF- $\kappa$ B that is critical in orchestrating the myelination program.<sup>28</sup>

So far, regulation of HDAC2 stability by ubiquitin–proteasome system has been documented. Basal and valproic acid (VPA)-induced HDAC2 turnover critically depend on the E2 ubiquitin conjugase Ubc8 and the E3 ubiquitin ligase RLIM.<sup>29</sup> Recently, MULE (Mcl-1 ubiquitin ligase E3, also named ARF-BP-1), a HECT domain ubiquitin ligase, was reported to specifically target HDAC2 for ubiquitination and degradation.<sup>30</sup> However, our knowledge about the regulation mechanism of HDAC2 is still limited.

In this study, we have identified ubiquitin-specific peptidase 4 (USP4) as a specific deubiquitinase of HDAC2. USP4-mediated deubiquitination and stabilization of HDAC2 inhibits p53 transcriptional and proapoptotic functions. Moreover, we found that USP4 targets HDAC2 to downregulate tumor necrosis factor- $\alpha$  (TNF $\alpha$ )-induced NF- $\kappa$ B activation. Therefore, our studies reveal USP4 suppresses p53 and NF- $\kappa$ B activation by stabilizing HDAC2.

<sup>1</sup>State Key Laboratory of Cellular Stress Biology and School of Life Sciences, Xiamen University, Xiamen, China; <sup>2</sup>Key Laboratory Breeding Base of Marine Genetic Resources, Third Institute of Oceanography, State Oceanic Administration, Xiamen, China; <sup>3</sup>Department of Radiotherapy, Changzhou Tumor Hospital, Soochow University, Changzhou, China; <sup>4</sup>School of Radiation Medicine and Protection and Collaborative Innovation Center of Radiation Medicine of Jiangsu Higher Education Institutions, Soochow University, Suzhou, China; <sup>5</sup>Zhongshan Hospital Xiamen University, Xiamen, China; <sup>6</sup>Division of Hematology, Children's Hospital of Philadelphia, Philadelphia, PA, USA and <sup>7</sup>Department of Pediatrics, Perelman School of Medicine at the University of Pennsylvania, Philadelphia, PA, USA. Correspondence: Dr J Chen, Key Laboratory Breeding Base of Marine Genetic Resources, Third Institute of Oceanography, State Oceanic Administration, Xiamen 361005 Fujian, China.

E-mail: chenjianming@tio.org.cn

<sup>8</sup>These authors contributed equally to this work.

Received 2 February 2015; revised 10 June 2015; accepted 10 August 2015; published online 28 September 2015

## RESULTS

### Identifying USP4 as a HDAC2-interacting protein

Deubiquitination is a process where ubiquitinated proteins can be reversed to counterbalance the ubiquitination process by cleaving ubiquitin from ubiquitin-conjugated protein substrates with the help of deubiquitinating enzymes such as USPs.<sup>31–34</sup> We postulated that USPs may be involved in the regulation of HDAC2. To this end, we generated a series of expression constructs encoding USPs. We tested the interaction between HDAC2 and USPs. Strong association of exogenous Myc-tagged USP4 with Flag-tagged HDAC2 was detected (Figure 1a). Furthermore, we sought to determine whether USP4 interacts with HDAC2 *in vivo*. Indeed, USP4 was detected in the anti-HDAC2 but not normal rabbit IgG immunoprecipitates from H1299 cell lysate (Figure 1b). Besides, the direct interaction between HDAC2 and USP4 was performed by the glutathione S-transferase (GST) pull-down assay. As shown in Figure 1c, GST-USP4 but not GST interacted with the full-length HDAC2.

To determine the region of HDAC2 involved in the interaction with USP4, two deletion mutants of HDAC2 were constructed (Figure 1e). As shown in Figure 1d, the N-terminal domain (amino acids 1–322) of HDAC2 was found to be sufficient for interaction with USP4, whereas the C-terminal domain (amino acids 322–488) showed no binding to USP4 (Figures 1d and e). To characterize the minimal region of USP4 essential for HDAC2 binding, we coexpressed various Myc-tagged USP4 truncation mutants with Flag-tagged HDAC2 in HEK-293T cells. Western blot analysis showed that 188–302 amino acids of USP4 retain the ability to coprecipitate Flag-tagged HDAC2 (Figures 1f and g).

To determine the cellular localization of USP4 and HDAC2 protein, the fusion constructs of Myc-USP4 and Flag-HDAC2 were co-transfected into H1299 cells. The proteins were detected by immunofluorescence. The results showed the nuclear distribution of both USP4 and HDAC2. USP4 protein colocalized with HDAC2 in the nuclei (Figure 1h). These results reveal that USP4 protein directly binds to HDAC2 in the nucleus.

### USP4 suppresses HDAC2 ubiquitination

USP4 contains a carboxyl-terminal ubiquitin hydrolase domain that defines the C-19 class of peptidases. Therefore, USP4 may regulate HDAC2 function via its deubiquitinase activity. To test this hypothesis, expression constructs encoding Flag-HDAC2, HA-Ub were co-transfected with empty vector control or expression constructs encoding Myc-USP4-WT or deubiquitinase-deficient C311A mutant into the HEK-293T cells. Cell lysates from the transfected cells were heated in the presence of 1% SDS and diluted with lysis buffer in order to disrupt noncovalent protein-protein interactions. Then, Flag-HDAC2 was immunoprecipitated with anti-Flag antibodies and immunoblotted with anti-HA for the detection of the ubiquitinated HDAC2. As shown in Figure 2a, overexpression of USP4-WT but not C311A mutant abrogated HDAC2 polyubiquitination. In contrast, USP11 failed to deubiquitinate HDAC2 (Figure 2b). Moreover, we generated H1299 cell lines stably expressing USP4 small hairpin RNA (shRNA) or control shRNA, followed by proteasome inhibitor MG132 treatment. HDAC2 ubiquitination was significantly increased in USP4 knockdown cells compared with the control cells. Reconstitution with shRNA-resistant USP4 restored HDAC2 ubiquitination, whereas USP4 C311A mutant cannot restore HDAC2 ubiquitination (Figure 2c).

To further confirm the above results, we analyzed the role of USP4 in the deubiquitination of HDAC2 *in vitro*. In this assay, Flag-HDAC2 proteins from HEK-293T cells were immunoprecipitated by Flag antibodies and then incubated with recombinant His-USP4-WT or -C311A mutant in the deubiquitination reaction buffer. The ubiquitination level of immunoprecipitated Flag-HDAC2 was found to be significantly decreased by incubation

with recombinant His-USP4-WT but not -C311A mutant proteins (Figure 2d). These results demonstrate that USP4 acts as an HDAC2 deubiquitinase.

### USP4 stabilizes HDAC2

As we demonstrated that USP4 deubiquitinates HDAC2, it is possible that USP4 can stabilize HDAC2. In fact, expression of USP4 significantly prolonged the half-life of HDAC2 (Figures 3a and b). The ubiquitin peptidase inactive form of USP4 (USP4-C311A) abolished its ability to stabilize HDAC2 (Figure 3c and Supplementary Figures S1A and B). Quantitative real-time reverse transcription (RT)-PCR analysis revealed that HDAC2 mRNA levels remained unchanged after USP4 expression (Figure 3d). Conversely, knockdown of endogenous USP4 expression facilitated HDAC2 protein degradation (Figure 3e), suggesting that USP4 stabilizes HDAC2. The MG132 rescued HDAC2 protein from degradation in USP4 knockdown cells (Figure 3e), indicating that polyubiquitination induces HDAC2 degradation through a proteasomal pathway. Quantitative real-time RT-PCR analysis revealed that HDAC2 mRNA levels were unchanged after knockdown of USP4 (Figure 3f). Collectively, our data indicate that USP4 deubiquitinates and stabilizes HDAC2 protein.

### USP4 inhibits p53 acetylation and transcriptional activity

Recently, HDAC2 was shown to suppress p53 hyperacetylation in embryonic epidermis.<sup>26</sup> In agreement with previous reports,<sup>35</sup> we found that HDAC2 could interact with p53 and inhibit the level of acetylated p53 (Supplementary Figures S2A and B). Because USP4 inhibits ubiquitination-mediated HDAC2 degradation, we hypothesized that USP4 inhibits p53 functions through HDAC2. In fact, our data show that USP4 inhibited the levels of acetylation but not protein expression of p53 (Figure 4a). Therefore, USP4 is a suppressor of p53 acetylation (K373/K382), a posttranslational modification that is required for p53 functions. As a consequence, USP4 inhibited p53-mediated luciferase activity in wild-type but not HDAC2 knockdown H1299 cells that were transfected with p53 (Figure 4b). Furthermore, we demonstrated that USP4 inhibited p53-mediated transcriptional activity in wild-type but not HDAC2 knockdown U2OS cells in response to DNA damage or not (Figures 4c and d). In contrast, silencing USP4 by shRNA remarkably increased the p53 activity in response to DNA damage or not (Figure 4e). We then tested whether USP4 expression inhibits cell apoptosis upon DNA damage. U2OS cells were transfected with either control or USP4 expression plasmids and then exposed to etoposide. Flow cytometry analysis indicated that USP4 expression suppressed etoposide-induced apoptosis, consistent with a previous report<sup>36</sup> (Figures 4f and g). Furthermore, knockdown of HDAC2 abolished the antiapoptotic functions of USP4, indicating that USP4 suppresses etoposide-induced apoptosis through HDAC2 (Figures 4f and g). Therefore, USP4 suppresses p53 transcriptional activity and proapoptotic functions.

### USP4 inhibits NF- $\kappa$ B transcriptional activity through HDAC2

Recent studies have shown that USP4 serves as a critical control to downregulate NF- $\kappa$ B activation through deubiquitinating TAK1, TRAF2 and TRAF6.<sup>37,38</sup> It has also been reported that HDAC2 could inhibit NF- $\kappa$ B activation.<sup>27,28</sup> In our study we found that HDAC2 could reduce TNF $\alpha$ -induced acetylation of RelA in H1299 cells, but HDAC2 could not interact with RelA (Supplementary Figures S3A and B), consistent with previous studies.<sup>27</sup> Therefore, we explored the possibility that USP4 inhibits NF- $\kappa$ B transcriptional activity through HDAC2 using an NF- $\kappa$ B-dependent luciferase reporter gene assay. As shown in Figure 5a, coexpression of wild-type USP4 significantly suppressed TNF $\alpha$ -mediated NF- $\kappa$ B activation. In contrast, knockdown of HDAC2 reduced the USP4 inhibitory

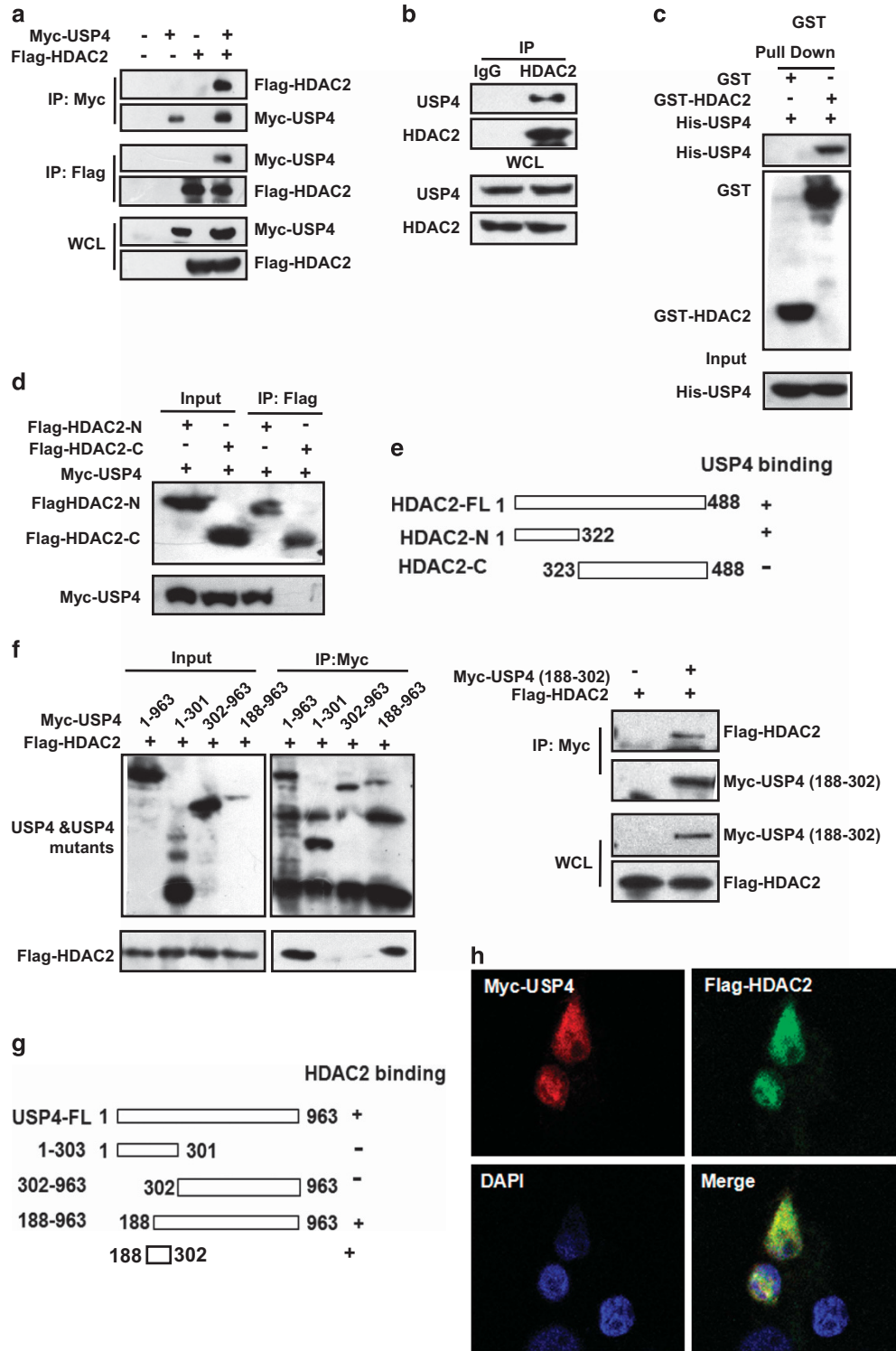


**Figure 1.** USP4 interacts with HDAC2. **(a)** The 293T cells were co-transfected with the indicated plasmids, and cell lysates were immunoprecipitated with the indicated antibodies and immunoblotted with anti-Flag or anti-Myc antibody. **(b)** Immunoprecipitation of HDAC2 from H1299 cells, followed by western blotting of the precipitated proteins with anti-HDAC2 and anti-USP4 antibodies. **(c)** *In vitro* binding assay. Purified His-USP4 (2  $\mu$ g) from *E. coli* BL21 was incubated with GST or GST-HDAC2 bound to glutathione-sepharose beads. Proteins retained on the beads were then blotted with the indicated antibodies. **(d)** Mapping of the HDAC2 domains responsible for binding to USP4. The 293T cells were co-transfected with Myc-USP4 and the indicated truncated Flag-HDAC2 mutants, and cell lysates were immunoprecipitated with anti-Flag antibody and immunoblotted with anti-Myc antibody. **(e)** Schematic representation of HDAC2 and HDAC2 deletion mutants used in the experiment in **(d)**. +, interaction; -, no interaction. **(f)** Mapping of the USP4 domains responsible for binding to HDAC2. The 293T cells were co-transfected with Flag-HDAC2 and the truncated Myc-USP4 mutants as indicated, and cell lysates were immunoprecipitated with anti-Myc antibody and then immunoblotted with anti-Flag antibody. **(g)** Schematic representation of USP4 and USP4 deletion mutants used in the experiment in **(f)**. +, interaction; -, no interaction. **(h)** Immunofluorescent detection of Flag-HDAC2 and Myc-USP4 in H1299 cells. Nuclei are counterstained by DAPI.

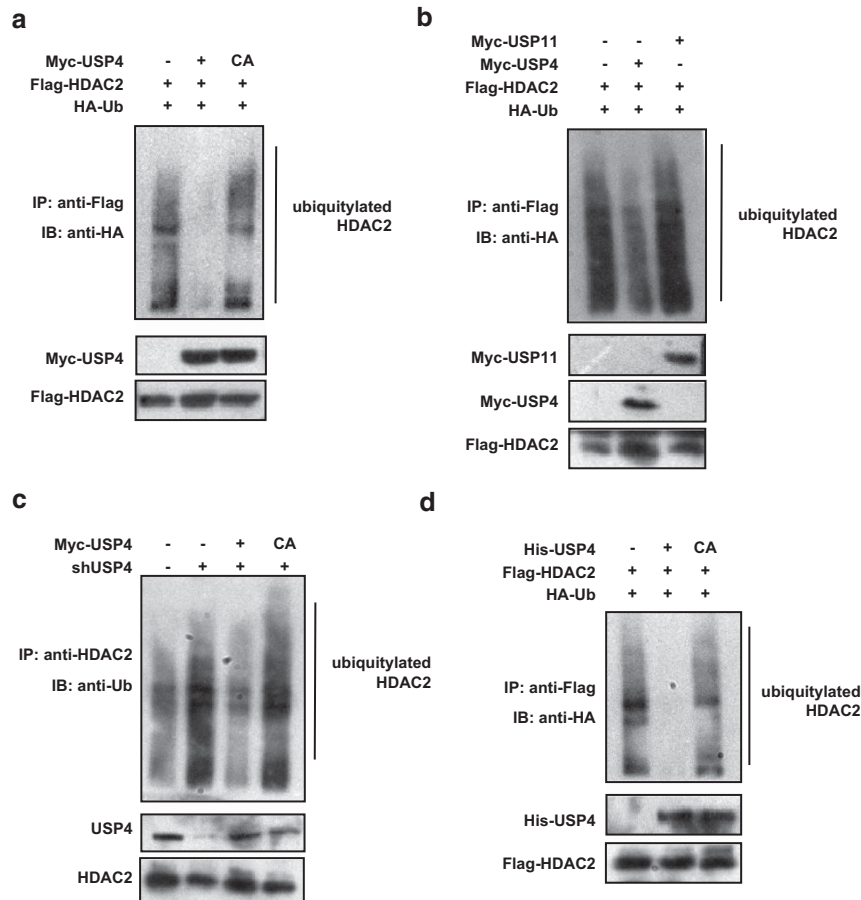


**Figure 2.** USP4 deubiquitinates HDAC2. **(a, b)** The 293T cells were transfected with the indicated combinations of expression vectors. Cells, 24 h after transfection, were treated with MG132 (5  $\mu$ M) for 3 h and then lysed. Cell lysates were immunoprecipitated with anti-Flag antibody (against Flag-HDAC2) and immunoblotted with anti-HA antibody (against HA-ubiquitin). **(c)** The H1299-control or H1299-USP4-RNAi cells were transfected with the indicated combinations of expression vectors. Cells, 24 h after transfection, were treated with MG132 (5  $\mu$ M) for 3 h and then lysed. Cell lysates were immunoprecipitated with anti-HDAC2 antibody and immunoblotted with anti-ubiquitin antibody. **(d)** Recombinant USP4 deubiquitinates HDAC2 *in vitro*. HEK-293T cells were transfected with expression vectors encoding Flag-HDAC2 and HA-ubiquitin. Cells were lysed in the lysis buffer only with phenylmethylsulfonyl fluoride (PMSF) as a protease inhibitor. Flag-HDAC2 proteins in the cell lysates were immunoprecipitated with anti-Flag antibodies and coincubated with purified recombinant His-USP4-WT or -C311A mutant for 2 h in the deubiquitination buffer before being analyzed by immunoblotting with the anti-HA antibodies.

effect on NF- $\kappa$ B activation. As a control, we found that USP4 and HDAC2 did not affect SV40 transcription activity (Supplementary Figure S3C). To determine further the role of USP4 on NF- $\kappa$ B target gene expression, we extracted total RNAs from the control and USP4-overexpression H1299 cells treated with TNF $\alpha$  and performed quantitative RT-PCR to examine the effect of overexpression of USP4 on TNF $\alpha$ -induced I $\kappa$ B $\alpha$  (Figure 5b). As shown in Figure 5c, knockdown of USP4 significantly enhanced the TNF $\alpha$ -mediated NF- $\kappa$ B activation. We sought to determine whether HDAC2 is involved in the USP4-mediated deubiquitination of TAK1 or TRAF2. Through the ubiquitin assay, we found that HDAC2 did not reflect the USP4-mediated deubiquitination of TAK1 or TRAF2 (Supplementary Figures S3D and E). These results suggest that deubiquitinating enzyme activity is responsible for the suppression of TNF $\alpha$ -mediated NF- $\kappa$ B activation by USP4. However, as shown in Supplementary Figure S3F, overexpression of USP4 did not significantly regulate TNF $\alpha$ -mediated apoptosis (Supplementary Figure S3F).

The expression of USP4 correlates with that of HDAC2 in cancer tissues

If the USP4-HDAC2 interaction enhances HDAC2 stability, then human tumors overexpressing USP4 protein might also

overexpress HDAC2. The expression levels of USP4 and HDAC2 proteins in a set of colorectal cancer tissues and the surrounding normal mucosal tissues were examined by western blot and immunohistochemistry. As determined by western blot analysis, levels of HDAC2 and USP4 protein were significantly upregulated in  $\sim$ 75% (9 out of 12) colorectal cancer tissues versus the surrounding normal mucosal tissues, and a positive correlation between the levels of USP4 and HDAC2 proteins was identified in colorectal cancer tissues (Figure 6a). Consistently, immunohistochemical staining of additional colorectal cancer tissues ( $n=12$ ) and normal mucosal tissue samples ( $n=12$ ; Figures 6b and c) showed that HDAC2 and USP4 levels were increased in the colorectal cancer tissues and the overall relationship between protein levels of USP4 and HDAC2 in the colorectal cancer samples was positively correlated significantly ( $r=0.62$ ;  $P<0.001$ ; Figures 6b and d), suggesting a malignant role of USP4 oversignaling in the occurrence and development of cancers through deubiquitinating and stabilizing HDAC2.

To determine whether p53 or NF- $\kappa$ B-responsive gene expression differed between colorectal cancers dependent on USP4 expression, p21 and I $\kappa$ B $\alpha$  expression was measured by RT-PCR from tumors analyzed in Figures 6a and b. Gene expression was



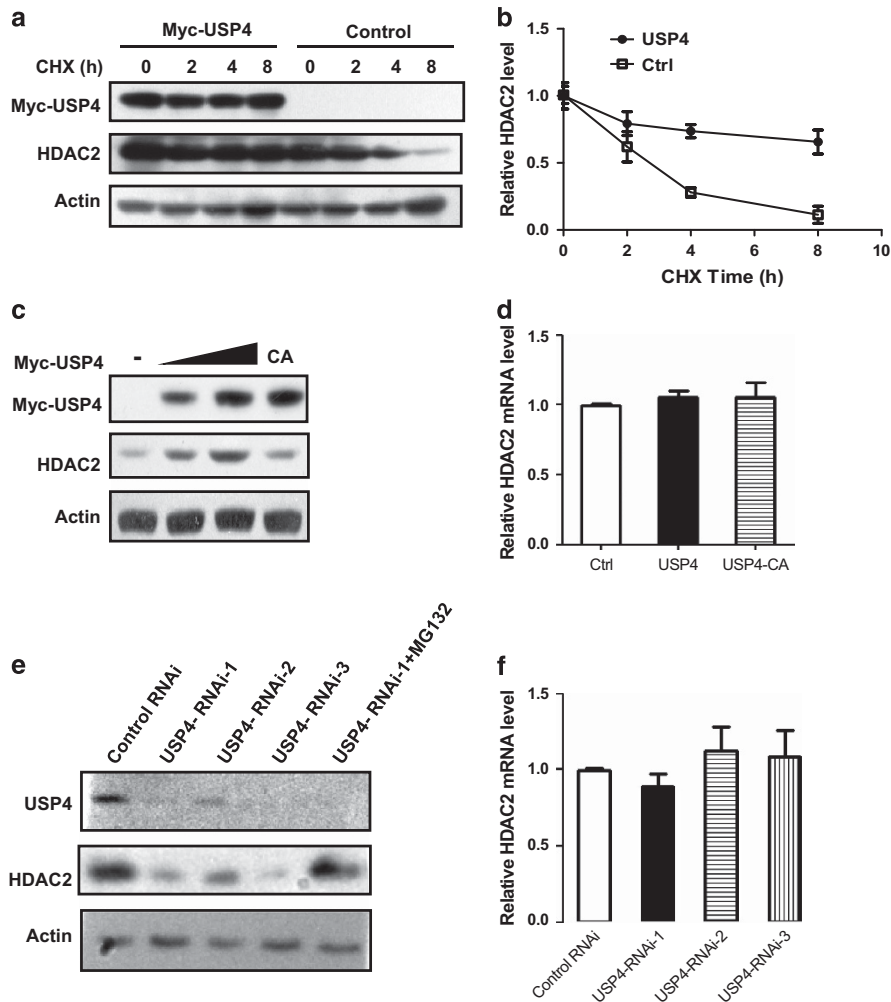


**Figure 3.** USP4 regulates HDAC2 turnover. **(a)** Half-life assay of endogenous HDAC2 protein. H1299 cells were transfected with vector or Myc-USP4 and then treated with 30  $\mu$ M/ml cycloheximide for the indicated durations and protein levels were detected by western blotting using anti-HDAC2, anti-Myc and anti-actin antibodies. **(b)** Quantification of the experiment. The values shown are obtained from three independent experiments and are normalized to the actin control. For each experimental condition, the signal at the start of the experiment was set to one. **(c)** The H1299 cells were transfected with increasing amounts of Myc-USP4 or -C311A mutant. Cell lysates were prepared 24 h post transfection and analyzed for the indicated proteins. **(d)** Quantitative real-time RT-PCR analysis of HDAC2 mRNA level. RNA was extracted from H1299-control and H1299-USP4 cells. HDAC2 mRNA was measured by quantitative RT-PCR, and levels relative to GAPDH mRNA are shown. Results are the mean  $\pm$  s.d. of three independent experiments. **(e)** Endogenous HDAC2 levels in control H1299 cells, USP4-RNAi H1299 cells or MG132-treated USP4-RNAi H1299 cells (5  $\mu$ M, 3 h) were analyzed by western blotting with the anti-HDAC2 or anti-USP4 antibodies. Actin was used as loading control. **(f)** Quantitative real-time RT-PCR analysis of HDAC2 mRNA level. RNA was extracted from control and USP4-RNAi H1299 cells. HDAC2 mRNA was measured by quantitative RT-PCR, and levels relative to GAPDH mRNA are shown. Results are the mean  $\pm$  s.d. of three independent experiments.

compared among the three groups of colorectal cancers with different USP4 protein levels: (1) similar USP4 expression compared with normal tissues ( $n = 9$ ) and (2) high USP4 expression ( $n = 15$ ) (Figures 6e and f). Data were normalized to assign median expression in normal tissues as 1. Compared with the group of colorectal cancers with USP4 protein levels similar to normal tissues, colorectal cancers with high USP4 protein contained significantly lower expression of p21 (Figure 6e). However, I $\kappa$ B $\alpha$  was elevated in all colorectal cancers compared with normal tissues but was not significantly different between the colorectal cancer groups based on USP4 expression (Figure 6f). Comparison of p21 and I $\kappa$ B $\alpha$  expression with USP4 protein levels measured within individual colorectal cancers revealed that increasing USP4 protein levels significantly correlated with decreased p21 expression (Spearman's correlation test,  $P < 0.05$ ). However, I $\kappa$ B $\alpha$  expression did not correlate with USP4 protein levels in colorectal cancers ( $P = 0.30$ ).

## DISCUSSION

This study demonstrates that USP4 is a deubiquitinase of HDAC2 and leads to suppression of both p53 and NF- $\kappa$ B transcriptional activity. This conclusion is supported by the following evidence. First, HDAC2 interacts with USP4 both *in vivo* and *in vitro*. Second, USP4 removes polyubiquitin chains that conjugate to and drive HDAC2 degradation through the proteasome pathway. Third, the USP4-mediated stabilization of HDAC2 leads to decreasing levels of p53 acetylation and suppression of p53-mediated transcriptional activity and apoptotic functions. The suppressive activity of USP4 on p53 functions depends on intact HDAC2 because USP4 failed to inhibit p53 transcriptional activity in HDAC2 knockdown cells. Fourth, USP4 inhibits NF- $\kappa$ B transcriptional activity through HDAC2. Finally, the expression of USP4 correlates with that of HDAC2 in cancer tissues.

A member of the USP family, USP4, has been observed to repress Toll-like receptor-, interleukin-1- and TNF $\alpha$ -induced NF- $\kappa$ B

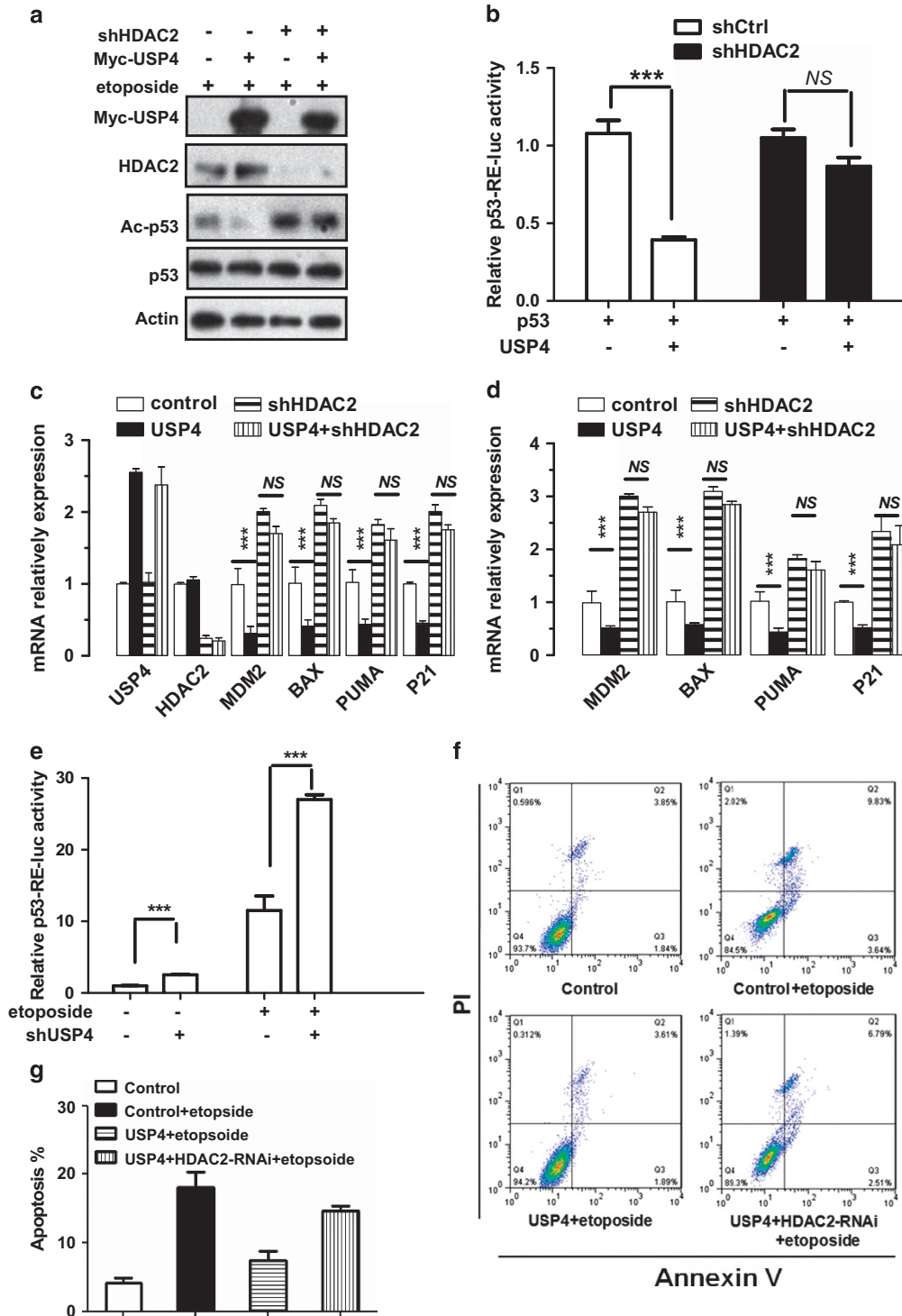


**Figure 4.** USP4 inhibits p53 acetylation and transcriptional activity. (a) H1299 cells were infected with lentiviruses expressing either control or shRNA targeting HDAC2 or transfected with USP4. After 48 h, cells were treated with 20  $\mu$ M of etoposide for 16 h. Cells were harvested and lysates were prepared for western blotting. The panels show immunoblots probed with the indicated antibodies. (b) H1299-control and H1299-HDAC2-RNAi cells were transfected with p53-RE-luciferase reporter. At 48 h post transfection, cells were transfected with p53 or not and luciferase activity was determined using a luciferase assay system. (c, d) Expression of USP4 HDAC2 MDM2 puma p21 Bax mRNA by quantitative RT-PCR. U2OS-control and U2OS-HDAC2-shRNA cells were transfected with USP4 or not and then treated with 20  $\mu$ M of etoposide for 16 h or not, and mRNA were extracted and subjected to quantitative RT-PCR. (e) U2OS-control and U2OS USP4-RNAi cells were treated with 20  $\mu$ M of etoposide or not. At 16 h post treatment, luciferase activity was determined using a luciferase assay system. (f, g) FACS analysis. U2OS-control and U2OS-HDAC2-shRNA cells were transfected with USP4 or not and then treated with 20  $\mu$ M of etoposide. After 24 h, cells were harvested, stained with propidium iodide (PI) and annexin V and the cell distribution was determined by flow cytometry. The percentage of cells in various phases of the cell is shown. Data are represented as mean  $\pm$  s.e.m. *P*-values were calculated using Student's *t*-test. \*\*\**P* < 0.001.

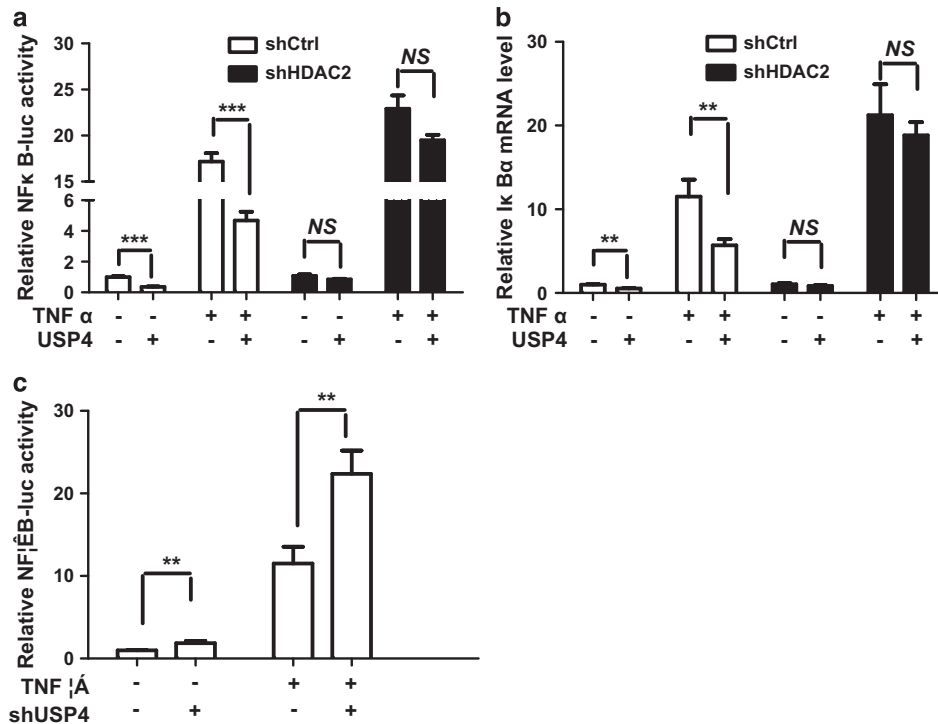


**Figure 5.** (a) H1299-control and H1299-HDAC2-shRNA cells were transfected with NF- $\kappa$ B luciferase reporter and USP4. At 48 h post transfection, cells were treated with 2 ng/ml TNF $\alpha$  or not and luciferase activity was determined using a luciferase assay system. (b) H1299-control and H1299-HDAC2-shRNA cells were transfected with USP4 or not. At 48 h post transfection, cells were treated with 2 ng/ml TNF $\alpha$  for 1 h or not, and mRNA was extracted and subjected to quantitative RT-PCR. (c) H1299-control and H1299-USP4-RNAi cells were treated with 2 ng/ml TNF $\alpha$  or not and luciferase activity was determined using a luciferase assay system. Data are represented as mean  $\pm$  s.e.m. *P*-values were calculated using Student's *t*-test. \*\**P* < 0.01; \*\*\**P* < 0.001.

activation by deubiquitinating K63-linked ubiquitin conjugates from TRAF2, TRAF6 and TAK1.<sup>37–39</sup> In addition to hydrolyzing K63-linked ubiquitination, USP4 also stabilizes molecules by deubiquitinating K48-linked ubiquitination. For example, USP4 interacts directly with and deubiquitinates ARF-binding protein 1 (ARF-BP1), leading to the stabilization of ARF-BP1 and subsequent reduction of p53 levels.<sup>36</sup> USP4 binds to and deubiquitinates the adenosine A2A receptor and enhances the cell surface level of the receptor.<sup>40</sup> As a deubiquitinating enzyme, USP4 was recently found to directly interact with type I transforming growth factor  $\beta$  receptor (T $\beta$ RI), leading to increases in the T $\beta$ RI level at the plasma membrane and in TGF $\beta$  signaling.<sup>41</sup> In this study, contrary to previous reports,<sup>36</sup> we did not see a noticeable effect of USP4 on the p53 level (Figure 4a). Different cell line or other factors may contribute to the discrepancy in the changes of p53 level upon loss or increase of USP4 function.

Recently, ARF-BP1 was reported to specifically target HDAC2 for ubiquitination and degradation and USP4 deubiquitinates and stabilizes ARF-BP1. Contrary to previous reports, we did not see a noticeable effect of the overexpression of USP4 on level of ARF-BP1 (Supplementary Figures S4A and B). However, differences in cell lines, knockdown efficiency or other factors may contribute to our inability to observe these changes in ARF-BP1 upon overexpression or knockdown of USP4. Nonetheless, USP4 might deubiquitinate and stabilize both ARF-BP1 and its substrate HDAC2. Numerous studies have demonstrated the existence of complicated HAUSP/MDM2/p53 feedback loop network that plays a very important role in the regulation of p53 stability. We hypothesize that the role of USP4 in the ARF-BP1 and HDAC2 is similar to the HAUSP/MDM2/p53 feedback loop. Both modes of regulation could potentially coexist to further fine-tune the control of expression in response to a variety of cellular stresses such as HDAC inhibitors.

We also sought to determine whether the interaction of USP4 and HDAC2 change following etoposide and TNF $\alpha$  stimulation. We found that the interaction between endogenous USP4 and HDAC2 did not change after etoposide and TNF $\alpha$  treatment (Supplementary Figure S5A). Previous studies have shown that the histone deacetylase inhibitor VPA could induce proteasomal degradation of HDAC2.<sup>29</sup> We detected the interaction between USP4 and HDAC2 after treatment with VPA. We also treated cells with MG132 that inhibits the proteasomal degradation of HDAC2. Remarkably, the interaction between endogenous USP4 and HDAC2 is significantly decreased upon VPA treatment. (Supplementary Figure S5B). Thus, the potential role of USP4 in biological processes in response to HDAC inhibitors such as VPA requires further investigation.

Several studies have shown that HDAC2 could inhibit NF- $\kappa$ B activity.<sup>27</sup> In our study we found that HDAC2 could reduce TNF $\alpha$ -induced acetylation of RelA in H1299 cells, but HDAC2 could not interact with RelA (Supplementary Figures S3A and B), consistent with previous studies.<sup>27</sup> In our studies, we found that I $\kappa$ B $\alpha$  mRNA level is higher in colorectal cancers than normal tissues. But the I $\kappa$ B $\alpha$  mRNA level did not correlate with USP4 protein level in colorectal cancer tissues (Figure 6f). This seems to be a controversy, as we all know that NF- $\kappa$ B activity and level are regulated by a complex network of regulators and at multiple levels.<sup>42,43</sup> Although USP4-HDAC2 appears to be an important player in regulating NF- $\kappa$ B activity, other regulators such as HDAC1 or p300 may be the primary regulators to maintain the physiological levels of NF- $\kappa$ B activity.<sup>27,44,45</sup> In addition, other USP4 or HDAC2 targets may also contribute to the regulation of NF- $\kappa$ B activity. The complex network of NF- $\kappa$ B regulators may partially explain the constitutively active NF- $\kappa$ B in many cancers, including colorectal cancer, in which USP4 and HDAC2 are highly expressed.

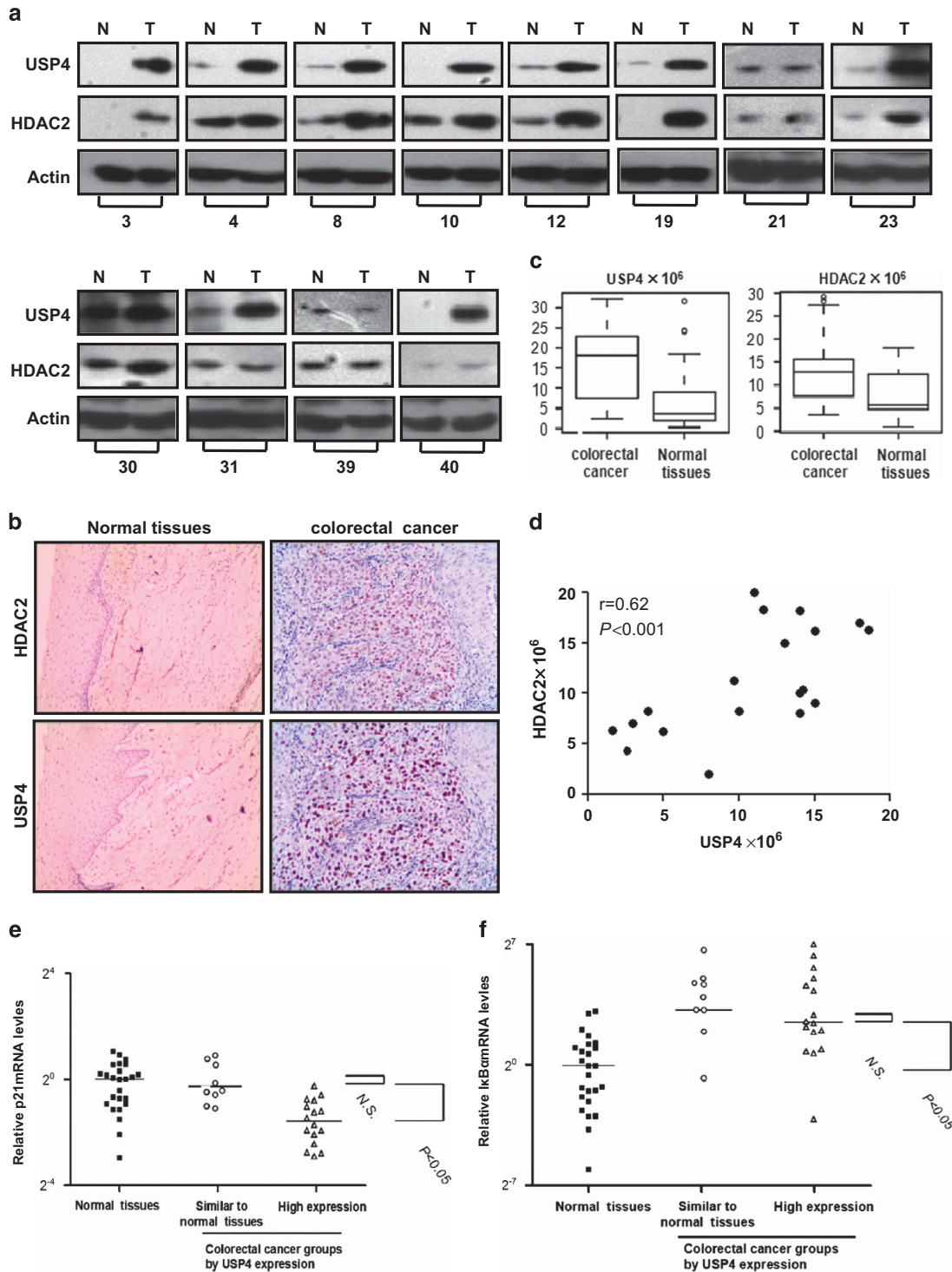


**Figure 6.** The expression of USP4 correlates with that of HDAC2 in cancer tissues. **(a)** Protein levels of USP4 and HDAC2 were determined by immunoblotting the protein extracts from tumor tissues (T) and their matched surrounding normal mucosal tissues (N). Actin was used as a loading control. **(b)** Representative immunohistochemical staining for USP4 and HDAC2 in colorectal cancer tissues ( $n=12$ ) and normal mucosal tissues ( $n=12$ ). **(c)** Box-and-whisker plots of the staining in **(b)** quantified by morphometry. Boxes represent the upper and lower quartiles and median; whiskers show the lowest data point within 1.5 interquartile range (IQR) from the lower quartile, and the highest data point within 1.5 IQR from the upper quartile. **(d)** Paired USP4 and HDAC2 staining intensities of colorectal cancer tissues samples in **(b)**. Spearman's rank correlation coefficient = 0.62;  $P < 0.001$ . The quantification data in **(c)** and **(d)** are expressed as the integrated DAB (3,3'-diaminobenzidine) intensity—that is, the sum of the light intensity of all pixels identified as 'brown' using an RGB threshold specific to DAB staining. **(e, f)** Total RNA was extracted from 24 pairs of tumors and normal surrounding tissues. Expressions of p21 and I $\kappa$ B $\alpha$  were determined by SYBR green-based quantitative real-time PCR using derived cDNA and corrected for input based on GAPDH expression. Data represent expression values of each gene relative to the median of expression in normal tissue (assigned as 1). Bars represented the median of each data set. Colorectal cancer was divided into two groups based on USP4 expression as described previously. The Mann-Whitney test was used to compare differences in expression of p21 and I $\kappa$ B $\alpha$  between colorectal cancer with higher USP4 expression and colorectal cancer with USP4 expression similar to normal tissues.



Compared with NF- $\kappa$ B, p53 turned out to be a *bona fide* target of HDAC2 in cancer cells. Numerous studies have shown that HDAC2 could directly interact with and inhibit p53 activity.<sup>35</sup> Our study show in Supplementary Figures S2A and B that HDAC2 could interact with p53 and reduce etoposide-induced acetylation of p53 in H1299 cells. We also found that the expression of p21, the target of p53, correlates with that of USP4 and HDAC2 in cancer tissues (Figure 6e). Hence, the USP4–HDAC2–p53 pathway may play a more important role in the development and progression of cancer than the USP4–HDAC2–NF- $\kappa$ B pathway that may take part in other biological processes such as inflammation. Thus, the potential role of USP4–HDAC2–NF- $\kappa$ B pathway in biological processes in response to different types of cell stresses requires further investigation.

HDAC2 is frequently observed to be highly expressed in human tumor tissues,<sup>46–48</sup> and overexpression of HDAC2 induces tumor cell proliferation, blocks apoptosis and promotes tumor progression.<sup>49–52</sup> Until recently, factors that induce HDAC2 overexpression were believed to be mediated mainly at the transcriptional level, including N-Myc and c-Myc oncoproteins.<sup>46,49</sup> However, the mechanisms underlying HDAC2 regulation now appear to be more complex than earlier conceptualized. An increasing number of studies provide evidence that HDAC2 expression is regulated at both the transcriptional and post-translational levels.<sup>29,30</sup> Of note, our studies show that USP4 deubiquitinates and stabilizes HDAC2 and the expression of USP4 correlates with that of HDAC2 in cancer tissues (Figures 6b and d). Several studies suggest that USP4 may be an oncogene and USP4 is overexpressed in a subset of human cancers. It will be of great interest to further examine the role of USP4–HDAC2 in the occurrence and development of cancers.

## MATERIALS AND METHODS

### Expression vectors

Full-length USP4 was amplified by PCR and subcloned into pCMV-Myc vector (Clontech, Mountain View, CA, USA). The pCMV-Myc-USP4 (C311A) mutant was generated with a QuikChange Lightning Site-Directed Mutagenesis Kit (Stratagene, Santa Clara, CA, USA). FLAG-tagged HDAC2 was PCR amplified and cloned into pCMV-Tag2 vector (Stratagene). USP4 and HDAC2 deletion mutants were constructed by PCR and inserted into their respective expression vectors. All constructs derived from PCR products were verified by DNA sequencing.

### Cell culture, transient transfection and treatments

Human H1299, U2OS, HEK293 and 293T cells were from ATCC (Manassas, VA, USA). All the cells were cultured in Dulbecco's modified Eagle's medium (Life Technologies, Carlsbad, CA, USA) supplemented with 10% fetal bovine serum (Hyclone, Logan, UT, USA) and 100  $\mu$ g/ml penicillin and streptomycin. Transient transfections were carried out using Lipofectamine 2000 (Invitrogen, Carlsbad, CA, USA). All the cells were tested for mycoplasma contamination.

### RNA interference

For RNA interference experiments we used a lentivirus-based vector, pLL3.7. Oligonucleotides targeting USP4 (USP4 shRNA-1, 5'-GAGATGCG GAAGCTATTCA-3'; USP4 shRNA-2, 5'-GAATCTGAGGCCTACGAGA-3'; USP4 shRNA-2, 5'-GACACCTTCACTTAGCAGT-3') or HDAC2 (HDAC2 shRNA, 5'-GTCTGCTACTACTACGACG-3') were cloned into the pLL3.7 vector. Recombinant lentiviral plasmids were co-transfected into 293T cells with the packaging plasmids VSV-G, RSV-REV and pMDL, and after 48 h the viral supernatants were used to infect target cells in the presence of 6  $\mu$ g/ml polybrene (Sigma-Aldrich, St Louis, MO, USA).

### Western blotting and immunoprecipitation

Total cell extracts were prepared in cell lysis buffer (20 mM Tris-HCl, pH 7.5, 150 mM NaCl, 10 mM NaF, 20 mM  $\beta$ -glycerophosphate, 1 mM sodium orthovanadate, 1 mM phenylmethylsulfonyl fluoride, 10  $\mu$ g/ml leupeptin, 2  $\mu$ g/ml aprotinin, 1% Triton X-100 and 1 mM EDTA) for

immunoprecipitations. Immunocomplexes were resolved by SDS–polyacrylamide gel electrophoresis, and western blotting was performed with the following antibodies: anti-Flag M2 (Sigma-Aldrich, F1804) and anti-actin (Sigma-Aldrich, A4700) monoclonal antibodies; HA (Y-11, SC-805), Myc (9E10, SC-40), Ub (P4D1, SC-8017), USP4 (H-3, SC-376000) and p53 (DO-1, SC-126) antibodies (Santa Cruz Biotechnology, Santa Cruz, CA, USA); acetylated p53 K373 (AB62376) antibody and anti-acetylated RelA (acetyl K310) (AB52175) (Abcam, Cambridge, MA, USA); (Upstate, Billerica, MA, USA); HDAC2 (12922-3-AP) antibodies (Proteintech, Wuhan, China); horseradish peroxidase-conjugated goat anti-mouse (32430) and anti-rabbit (31210) (Thermo Scientific, Waltham, MA, USA); and ARF-BP1 antibodies (A300-486A, Bethyl, Montgomery, TX, USA).

### Quantitative real-time RT-PCR

Total RNA was isolated from cells using RNA Simple Total RNA Kit (Tiangen Biotech, Beijing, China), and first-strand complementary DNA (cDNA) was synthesized from 1  $\mu$ g of total RNA using the First-Strand cDNA Synthesis kit (Toyobo, Osaka, Japan) following the manufacturer's instructions. Prepared cDNA samples were amplified and analyzed by quantitative real-time RT-PCR with Power SYBR Green PCR Master Mix (Applied Biosystems, Foster City, CA, USA) using ABI 7500 Real-Time PCR System (Applied Biosystems). Primer sequences were as follows: human USP4, 5'-AAGG AAGCTGGGAGAAT-3' (forward) and 5'-GCAGTGGCAGCGTTAGAT-3' (reverse); human HDAC2, 5'-ATATTGTGCTTGCCATCC-3' (forward) and 5'-CTCAAGTCTCTGTGCC-3' (reverse); human MDM2, 5'-AGGGAAG AAACCAAGAC-3' (forward) and 5'-TAAAGCAGGCCATAAGAT-3' (reverse); human p21, 5'-TGGCACCTCACCTGCTCTG-3' (forward) and 5'-CGGCGT TTGGAGTGGTAGAA-3' (reverse); human BAX, 5'-ATCGAGCAGGCGGAATG-3' (forward) and 5'-TGTCACGGCGGCAAT-3' (reverse); human PUMA, 5'-CGG CGGAGACAAGAGGAGC-3' (forward) and 5'-CAGGGTGTGAGGAGTGGGAG-3' (reverse); human I $\kappa$ B $\alpha$ , 5'-CCAGGCTATTCTCCCTACC-3' (forward) and 5'-CTTTGCGCTATAACGTAGC-3' (reverse); human GAPDH, 5'-GACATCA AGAAGTGGTGAA-3' (forward) and 5'-TGTCATACCGAAATGAGC-3' (reverse).

### GST pull-down assays

*Escherichia coli* BL21 harboring expression vectors for GST-HDAC2, His-USP4 or GST alone and His-USP4 were grown to A600=0.6–0.8 and induced with isopropyl  $\beta$ -D-1-thiogalactopyranoside for 6 h. Purified His-USP4 from *E. coli* BL21 was incubated with GST or GST-HDAC2 bound to glutathione–sepharose beads. The beads were collected by centrifugation and washed five times with phosphate-buffered saline. Proteins retained on the beads were then blotted with the anti-His antibody (1:500; Santa Cruz Biotechnology).

### Luciferase assays

U2OS cells were transfected with either a p53-RE or 3\*Kb promoter-driven luciferase construct, and a control *Renilla* luciferase construct using Lipofectamine 2000. Cells were incubated for 24 h and then treated with 20  $\mu$ M of etoposide for 16 h or TNF $\alpha$  (2 ng/ml) for 6 h. Luciferase activity was determined with the Dual Luciferase System (Promega, San Luis Obispo, CA, USA) following the manufacturer's instructions.

### In vivo ubiquitination assay

Cells were co-transfected with expression vectors of Myc-USP4, HA-ubiquitin and Flag-HDAC2. At 36 h after transfection, cells were treated with 5  $\mu$ M MG132 for 3 h before being harvested. Then, cells were lysed with RIPA buffer (0.5% SDS, 0.5% sodium deoxycolate, 0.5% Nonidet P-40, 150 mM NaCl, 10 mM NaF, 20 mM  $\beta$ -glycerophosphate, 1 mM sodium orthovanadate, 1 mM phenylmethylsulfonyl fluoride, 10  $\mu$ g/ml leupeptin and 2  $\mu$ g/ml aprotinin), followed by incubation with Flag antibodies overnight at 4°C and incubated with Protein G sepharose beads for another 4 h. The immunoprecipitates were boiled in SDS buffer and subjected to western blotting analysis. HDAC2 proteins were immunoprecipitated by Flag antibodies and ubiquitinated HDAC2 was detected by anti-HA antibody.

### In vitro deubiquitination assay

To perform *in vitro* deubiquitination assay, Flag-HDAC2 expression vectors were transfected into HEK-293T cells with the vectors encoding HA-Ub. Flag-HDAC2 proteins in the cell lysates were immunoprecipitated with

anti-Flag antibodies and coincubated with purified recombinant His-USP4-WT or -C311A mutant for 2 h at 30 °C in a final volume of 20  $\mu$ l of deubiquitination buffer (30 mM Tris (pH 7.6), 10 mM KCl, 5 mM MgCl<sub>2</sub>, 5% glycerol, 5 mM DTT and 2 mM ATP). The reaction mixtures were resolved by SDS-polyacrylamide gel electrophoresis and then analyzed by immunoblotting with the anti-Ub antibodies.

### Immunohistochemistry

For immunohistochemistry staining and scoring, tissues were fixed in 10% neutral buffered formalin and later embedded in paraffin. Then, 3  $\mu$ m thick paraffin sections were deparaffinized and heat treated with citrate buffer, pH 6.0, for 7 min as an epitope retrieval protocol. Endogenous peroxidase was blocked with 3% hydrogen peroxide for 15 min at room temperature, and tissue nonspecific-binding sites were blocked with skimmed milk powder at 4% applied for 30 min. Sections were then incubated with the USP4 and HDAC2 antibodies for 1 h (dilution 1:200) and mixed with skimmed milk powder at 2% again to reduce unspecific staining. Biotinylated secondary antibody was then added for 30 min. Avidin-biotin-peroxidase complex (Dako LSAB2 system, DAKO Co., Carpinteria, CA, USA) was added and color was developed using 3'-3'-diaminobenzidine. Counterstaining was done with hematoxylin. All steps were performed at room temperature.

### Tissue samples

Tissue samples were collected from 24 patients who had not received chemotherapy or radiotherapy before surgery in 2014. All patients gave signed, informed consent for their tissues to be used for scientific research. Ethical approval for the study was obtained from the Changzhou Tumor Hospital, Soochow University.

### Data analysis

For data analysis, cells or tissues were randomly allocated to treatment groups, and images were picked randomly. The investigators assessing, measuring or quantifying experimental outcomes were double-blinded to the group allocation.

For co-immunoprecipitation, luciferase assay or mRNA relative expression, three (or at least three) independent experiments were performed. For immunohistochemical staining, 12 samples from colorectal cancer tissues and normal colorectal tissues were analyzed. For p21 and I $\kappa$ B $\alpha$  expression experiments, 24 samples from colorectal cancer tissues and normal colorectal tissues were analyzed. The estimate of variation within each group of data was carried out by F-test, and each variance between the compared groups is similar. The correlation test was performed by Spearman's correlation test. The other statistical analyses were performed by unpaired Student's *t*-test.

### CONFLICT OF INTEREST

The authors declare no conflict of interest.

### ACKNOWLEDGEMENTS

We thank all the members of the Jianming Chen laboratory for their help and assistance. This work was supported by the Scientific Research Foundation of Third Institute of Oceanography, SOA (No. 2015011), DY125-15-T-03 from China Ocean Mineral Resources R&D Association, the National Natural Science Foundation of China (81402518), grants from China Postdoctoral Science Foundation (No. 2013M541853), China Postdoctoral Science Foundation (No. 2014T70606), Marine Public Welfare Project 201005022, the National Science Foundation grant 31171366, the Scientific Research Foundation of Third Institute of Oceanography, SOA (No. 2014007), the National Natural Science Foundation of China (41201531), China Ocean Mineral Resources R&D Association (DY-125-15-T-08), the National Natural Science Foundation of China (31272684), special financial fund of innovative development of marine economic demonstration project, GD2012-D01-001.

### REFERENCES

- Bolden JE, Peart MJ, Johnstone RW. Anticancer activities of histone deacetylase inhibitors. *Nat Rev Drug Discov* 2006; **5**: 769–784.
- de Ruijter AJ, van Gennip AH, Caron HN, Kemp S, van Kuilenburg AB. Histone deacetylases (HDACs): characterization of the classical HDAC family. *Biochem J* 2003; **370**: 737–749.

- Blander G, Guarente L. The Sir2 family of protein deacetylases. *Annu Rev Biochem* 2004; **73**: 417–435.
- Strahl BD, Allis CD. The language of covalent histone modifications. *Nature* 2000; **403**: 41–45.
- Haberland M, Montgomery RL, Olson EN. The many roles of histone deacetylases in development and physiology: implications for disease and therapy. *Nat Rev Genet* 2009; **10**: 32–42.
- Gong F, Miller KM. Mammalian DNA repair: HATs and HDACs make their mark through histone acetylation. *Mutat Res* 2013; **750**: 23–30.
- Yang XJ, Seto E. HATs and HDACs: from structure, function and regulation to novel strategies for therapy and prevention. *Oncogene* 2007; **26**: 5310–5318.
- Segre CV, Chiocca S. Regulating the regulators: the post-translational code of class I HDAC1 and HDAC2. *J Biomed Biotechnol* 2011; **2011**: 690848.
- Glozak MA, Sengupta N, Zhang X, Seto E. Acetylation and deacetylation of non-histone proteins. *Gene* 2005; **363**: 15–23.
- Luo J, Su F, Chen D, Shiloh A, Gu W. Deacetylation of p53 modulates its effect on cell growth and apoptosis. *Nature* 2000; **408**: 377–381.
- Vaziri H, Dessain SK, Ng Eaton E, Imai SI, Frye RA, Pandita TK et al. hSIR2(SIRT1) functions as an NAD-dependent p53 deacetylase. *Cell* 2001; **107**: 149–159.
- Sykes SM, Mellert HS, Holbert MA, Li K, Marmorstein R, Lane WS et al. Acetylation of the p53 DNA-binding domain regulates apoptosis induction. *Mol Cell* 2006; **24**: 841–851.
- Tang Y, Luo J, Zhang W, Gu W. Tip60-dependent acetylation of p53 modulates the decision between cell-cycle arrest and apoptosis. *Cell* 2006; **24**: 827–839.
- Horn HF, Vousden KH. Coping with stress: multiple ways to activate p53. *Oncogene* 2007; **26**: 1306–1316.
- Vousden KH, Lane DP. p53 in health and disease. *Nat Rev Mol Cell Biol* 2007; **8**: 275–283.
- Levine AJ. p53, the cellular gatekeeper for growth and division. *Cell* 1997; **88**: 323–331.
- Shieh SY, Ikeda M, Taya Y, Prives C. DNA damage-induced phosphorylation of p53 alleviates inhibition by MDM2. *Cell* 1997; **91**: 325–334.
- Li M, Luo J, Brooks CL, Gu W. Acetylation of p53 inhibits its ubiquitination by Mdm2. *J Biol Chem* 2002; **277**: 50607–50611.
- Feng L, Lin T, Uranishi H, Gu W, Xu Y. Functional analysis of the roles of posttranslational modifications at the p53 C terminus in regulating p53 stability and activity. *Mol Cell Biol* 2005; **25**: 5389–5395.
- Menendez D, Inga A, Resnick MA. The expanding universe of p53 targets. *Nat Rev Cancer* 2009; **9**: 724–737.
- Bekerman R, Prives C. Transcriptional regulation by p53. *Cold Spring Harb Perspect Biol* 2010; **2**: a000935.
- Lakin ND, Jackson SP. Regulation of p53 in response to DNA damage. *Oncogene* 1999; **18**: 7644–7655.
- Gu W, Roeder RG. Activation of p53 sequence-specific DNA binding by acetylation of the p53 C-terminal domain. *Cell* 1997; **90**: 595–606.
- Vogelstein B, Lane D, Levine AJ. Surfing the p53 network. *Nature* 2000; **408**: 307–310.
- Juan LJ, Shia WJ, Chen MH, Yang WM, Seto E, Lin YS et al. Histone deacetylases specifically down-regulate p53-dependent gene activation. *J Biol Chem* 2000; **275**: 20436–20443.
- LeBoeuf M, Terrell A, Trivedi S, Sinha S, Epstein JA, Olson EN et al. Hdac1 and Hdac2 act redundantly to control p63 and p53 functions in epidermal progenitor cells. *Dev Cell* 2010; **19**: 807–818.
- Ashburner BP, Westerheide SD, Baldwin AS Jr. The p65 (RelA) subunit of NF- $\kappa$ B interacts with the histone deacetylase (HDAC) corepressors HDAC1 and HDAC2 to negatively regulate gene expression. *Mol Cell Biol* 2001; **21**: 7065–7077.
- Chen Y, Wang H, Yoon SO, Xu X, Hottiger MO, Svaren J et al. HDAC-mediated deacetylation of NF- $\kappa$ B is critical for Schwann cell myelination. *Nat Neurosci* 2011; **14**: 437–441.
- Kramer OH, Zhu P, Ostendorff HP, Golebiewski M, Tiefenbach J, Peters MA et al. The histone deacetylase inhibitor valproic acid selectively induces proteasomal degradation of HDAC2. *EMBO J* 2003; **22**: 3411–3420.
- Zhang J, Kan S, Huang B, Hao Z, Mak TW, Zhong Q. Mule determines the apoptotic response to HDAC inhibitors by targeted ubiquitination and destruction of HDAC2. *Genes Dev* 2011; **25**: 2610–2618.
- Nijman SM, Luna-Vargas MP, Velds A, Brummelkamp TR, Dirac AM, Sixma TK et al. A genomic and functional inventory of deubiquitinating enzymes. *Cell* 2005; **123**: 773–786.
- Amerik AY, Hochstrasser M. Mechanism and function of deubiquitinating enzymes. *Biochim Biophys Acta* 2004; **1695**: 189–207.
- Baek KH. Cytokine-regulated protein degradation by the ubiquitination system. *Curr Protein Pept Sci* 2006; **7**: 171–177.
- Ramakrishna S, Suresh B, Baek KH. The role of deubiquitinating enzymes in apoptosis. *Cell Mol Life Sci* 2011; **68**: 15–26.
- Wagner T, Brand P, Heinzel T, Kramer OH. Histone deacetylase 2 controls p53 and is a critical factor in tumorigenesis. *Biochim Biophys Acta* 2014; **1846**: 524–538.

- 36 Zhang X, Berger FG, Yang J, Lu X. USP4 inhibits p53 through deubiquitinating and stabilizing ARF-BP1. *EMBO J* 2011; **30**: 2177–2189.
- 37 Fan YH, Yu Y, Mao RF, Tan XJ, Xu GF, Zhang H *et al*. USP4 targets TAK1 to downregulate TNF $\alpha$ -induced NF- $\kappa$ B activation. *Cell Death Differ* 2011; **18**: 1547–1560.
- 38 Xiao N, Li H, Luo J, Wang R, Chen H, Chen J *et al*. Ubiquitin-specific protease 4 (USP4) targets TRAF2 and TRAF6 for deubiquitination and inhibits TNF $\alpha$ -induced cancer cell migration. *Biochem J* 2012; **441**: 979–986.
- 39 Zhou F, Zhang X, van Dam H, Ten Dijke P, Huang H, Zhang L. Ubiquitin-specific protease 4 mitigates Toll-like/interleukin-1 receptor signaling and regulates innate immune activation. *J Biol Chem* 2012; **287**: 11002–11010.
- 40 Milojevic T, Reiterer V, Stefan E, Korkhov VM, Dorostkar MM, Ducza E *et al*. The ubiquitin-specific protease Usp4 regulates the cell surface level of the A2A receptor. *Mol Pharmacol* 2006; **69**: 1083–1094.
- 41 Zhang L, Zhou F, Drabsch Y, Gao R, Snaar-Jagalska BE, Mickanin C *et al*. USP4 is regulated by AKT phosphorylation and directly deubiquitylates TGF- $\beta$  type I receptor. *Nat Cell Biol* 2012; **14**: 717–726.
- 42 Chang AA, Van Waes C. Nuclear factor- $\kappa$ B as a common target and activator of oncogenes in head and neck squamous cell carcinoma. *Adv Otorhinolaryngol* 2005; **62**: 92–102.
- 43 Chung CH, Parker JS, Ely K, Carter J, Yi Y, Murphy BA *et al*. Gene expression profiles identify epithelial-to-mesenchymal transition and activation of nuclear factor- $\kappa$ B signaling as characteristics of a high-risk head and neck squamous cell carcinoma. *Cancer Res* 2006; **66**: 8210–8218.
- 44 Zhong H, May MJ, Jimi E, Ghosh S. The phosphorylation status of nuclear NF- $\kappa$ B determines its association with CBP/p300 or HDAC-1. *Mol Cell* 2002; **9**: 625–636.
- 45 Rocha S, Campbell KJ, Perkins ND. p53- and Mdm2-independent repression of NF- $\kappa$ B transactivation by the ARF tumor suppressor. *Mol Cell* 2003; **12**: 15–25.
- 46 Marshall GM, Gherardi S, Xu N, Neiron Z, Trahair T, Scarlett CJ *et al*. Transcriptional upregulation of histone deacetylase 2 promotes Myc-induced oncogenic effects. *Oncogene* 2010; **29**: 5957–5968.
- 47 Weichert W, Roske A, Niesporek S, Noske A, Buckendahl AC, Dietel M *et al*. Class I histone deacetylase expression has independent prognostic impact in human colorectal cancer: specific role of class I histone deacetylases in vitro and in vivo. *Clin Cancer Res* 2008; **14**: 1669–1677.
- 48 Fritsche P, Seidler B, Schuler S, Schnieke A, Gottlicher M, Schmid RM *et al*. HDAC2 mediates therapeutic resistance of pancreatic cancer cells via the BH3-only protein NOXA. *Gut* 2009; **58**: 1399–1409.
- 49 Zhu P, Martin E, Mengwasser J, Schlag P, Janssen KP, Gottlicher M. Induction of HDAC2 expression upon loss of APC in colorectal tumorigenesis. *Cancer Cell* 2004; **5**: 455–463.
- 50 Huang BH, Laban M, Leung CH, Lee L, Lee CK, Salto-Tellez M *et al*. Inhibition of histone deacetylase 2 increases apoptosis and p21Cip1/WAF1 expression, independent of histone deacetylase 1. *Cell Death Differ* 2005; **12**: 395–404.
- 51 Hrzenjak A, Moinfar F, Kremser ML, Strohmeier B, Staber PB, Zatloukal K *et al*. Valproate inhibition of histone deacetylase 2 affects differentiation and decreases proliferation of endometrial stromal sarcoma cells. *Mol Cancer Ther* 2006; **5**: 2203–2210.
- 52 Heideman MR, Wilting RH, Yanover E, Velds A, de Jong J, Kerkhoven RM *et al*. Dosage-dependent tumor suppression by histone deacetylases 1 and 2 through regulation of c-Myc collaborating genes and p53 function. *Blood* 2013; **121**: 2038–2050.



This work is licensed under a Creative Commons Attribution-NonCommercial-ShareAlike 4.0 International License. The images or other third party material in this article are included in the article's Creative Commons license, unless indicated otherwise in the credit line; if the material is not included under the Creative Commons license, users will need to obtain permission from the license holder to reproduce the material. To view a copy of this license, visit <http://creativecommons.org/licenses/by-nc-sa/4.0/>

Supplementary Information accompanies this paper on the Oncogene website (<http://www.nature.com/onc>)